Drug Deliv. and Transl. Res. (2018) 8:329–341
DOI 10.1007/s13346-017-0377-4

ORIGINAL ARTICLE

Chemopreventive efficacy of curcumin-loaded PLGA microparticles in a transgenic mouse model of HER-2-positive breast cancer

Alex E. Grill [1,2] · **Komal Shahani** [1] · **Brenda Koniar** [3] · **Jayanth Panyam** [1,2]

Published online: 17 April 2017

Abstract Curcumin has shown promising inhibitory activity against HER-2-positive tumor cells in vitro but suffers from poor oral bioavailability in vivo. Our lab has previously developed a polymeric microparticle formulation for sustained delivery of curcumin for chemoprevention. The goal of this study was to examine the anticancer efficacy of curcumin-loaded polymeric microparticles in a transgenic mouse model of HER-2 cancer, Balb-*neu*T. Microparticles were injected monthly, and mice were examined for tumor appearance and growth. Initiating curcumin microparticle treatment at 2 or 4 weeks of age delayed tumor appearance by 2–3 weeks compared to that in control mice that received empty microparticles. At 12 weeks, abnormal (lobular hyperplasia, carcinoma in situ, and invasive carcinoma) mammary tissue area was significantly decreased in curcumin microparticle-treated mice, as was CD-31 staining. Curcumin treatment decreased mammary VEGF levels significantly, which likely contributed to slower tumor formation. When compared to saline controls, however, blank microparticles accelerated tumorigenesis and curcumin treatment abrogated this effect, suggesting that PLGA microparticles enhance tumorigenesis in this model. PLGA microparticle administration was shown to be associated with higher plasma lactic acid levels and increased activation of NF-κB. The unexpected side effects of PLGA microparticles may be related to the high dose of the microparticles that was needed to achieve sustained curcumin levels in vivo. Approaches that can decrease the overall dose of curcumin (for example, by increasing its potency or reducing its clearance rate) may allow the development of sustained release curcumin dosage forms as a practical approach to cancer chemoprevention.

Keywords Cancer chemoprevention · Sustained release · Polymeric microparticles · Tumorigenesis · Inflammation

Introduction

Human epidermal growth factor receptor-2 (HER-2), a membrane receptor tyrosine kinase, is an upstream effector of Ras, Akt, and NF-κB [1–3]. Overexpression of HER-2 leads to dysregulation of cellular division as well as induction of inflammation. Patients who have HER-2+ tumors are at high risk for metastases in the lung, bone, and brain [4, 5]. Availability of targeted therapies (the HER-2-targeted monoclonal antibody, trastuzumab, and the receptor tyrosine kinase inhibitor, lapatinib) has improved the 5-year survival rate in these patients [6–8]. However, these targeted therapies do not cross the blood-brain barrier effectively, making it difficult to treat brain metastases [9, 10]. In addition, HER-2+ breast cancer is associated with higher incidence of recurrence [11]. Therefore, a chemopreventive approach to HER-2+ breast cancer would be highly valuable.

Curcumin induces HER-2 ubiquitination and subsequent degradation resulting in the inhibition of HER-2+ tumor cells [12, 13]. Curcumin's other anticancer effects mainly stem from inhibition of NF-κB activation [14–16]. Despite promising preclinical studies, the use of curcumin in the clinic has been severely limited by its very low bioavailability [17].

✉ Jayanth Panyam
jpanyam@umn.edu

[1] Department of Pharmaceutics, College of Pharmacy, University of Minnesota, 9-177 Weaver Densford Hall, 308 Harvard Street, S.E, Minneapolis, MN 55455, USA

[2] Masonic Cancer Research Center, University of Minnesota, Minneapolis, MN 55455, USA

[3] Research Animal Resources, University of Minnesota, Minneapolis, MN 55455, USA

Injectable microparticle (microparticles)-based drug delivery offers the ability to bypass gut absorption and first pass metabolism [18–21]. Formulation parameters can be fine-tuned to sustain drug plasma levels over a course of weeks to months depending on the excipients used [20]. Our laboratory has previously developed an injectable microparticle formulation using the FDA-approved polymer, poly(lactide-*co*-glycolic acid) (PLGA), for sustained curcumin delivery [22, 23]. This formulation maintained curcumin blood levels for at least 1 month and effectively inhibited tumor growth in a mouse xenograft MDA-MB-231 model of triple negative breast cancer.

The goal of the current study was to examine the efficacy of curcumin-loaded PLGA microparticles in a transgenic mouse model of HER-2+ breast cancer, Balb-*neu*T. Mice were treated with curcumin-loaded microparticles beginning at varying time points in tumor progression to determine the optimal time of intervention. The effect of curcumin treatment on tumor multiplicity, growth, and angiogenesis was determined.

Materials and methods

Materials

PLGA (50:50, intrinsic viscosity = 0.95–1.20 dL/g) was purchased from LACTEL Absorbable Polymers (Birmingham, AL). High-purity curcumin (>98% curcuminoids), casein, Tween 80, and polyvinyl alcohol (PVA, 30–70 kDa MW) were purchased from Sigma-Aldrich (St. Louis, MO). Acetonitrile, methanol, and chloroform were purchased from Fisher Scientific (Pittsburg, PA). Anti-HER-2 and anti-VEGF antibodies were purchased from Santa Cruz Biotechnology (Santa Cruz, CA). Anti-β-tubulin antibody and HRP-linked anti-rabbit IgG were purchased from Cell Signaling Technology (Beverly, MA). HRP-linked anti-β-actin antibody was purchased from Sigma-Aldrich; 1× RIPA buffer, endotoxin-free water, and SuperSignal West Pico Chemiluminescent Substrate were purchased from Thermo Scientific (Waltham, MA).

Microparticle fabrication

Curcumin-loaded microparticles were prepared using a rapid solvent evaporation technique published previously [22, 23]. Briefly, curcumin (20 mg) and PLGA (20 mg) were dissolved in 1.65 mL of chloroform-methanol mixture (10:1 *v/v*). This solution was emulsified in 6 mL of 2% *w/v* PVA for 2 min using a digital vortex (FisherSci) set at 1000 rpm. Chloroform was removed from the emulsion over 25 min using a benchtop rotary evaporator (Heidolph, Schwabach, Germany). Particles were collected by centrifugation and washed twice with 10% *w/v* Tween 80 and then twice with water to remove unencapsulated curcumin [22, 23]. Particles were then lyophilized for 48 h (Labconco, Kansas City, MO). Nondrug-loaded (blank) PLGA microparticles were prepared similarly but without curcumin. Endotoxin-free water was used for preparing all the aqueous solutions. Curcumin content was measured by extracting a known amount of curcumin-loaded microparticles with methanol at room temperature overnight on a rotary extractor. The suspension was centrifuged at 20,000×*g* for 10 min (Eppendorf, Hamburg, Germany) and the supernatant was analyzed by HPLC. HPLC was performed on a Beckman HPLC system connected to a PDA detector (Brea, CA). Curcumin was eluted on a XDB-C18 Agilent column (250 × 4.6 mm, 5 μm) (Santa Clara, CA). Mobile phase consisted of 10 mM ammonium acetate (pH 4, adjusted with glacial acetic acid) and acetonitrile (35:65) run isocratically at 1 mL/min. Curcumin (λ_{max} = 430 nm) eluted at 4.9 min. Curcumin produced a linear standard plot over the range of 1.56–25 μg/mL with a R^2 >0.999. Drug loading (% *w/w*) was calculated by dividing the amount of curcumin encapsulated in microparticles by the amount of microparticles and multiplying by 100. Encapsulation efficiency (%) was calculated as the percent of added curcumin that was successfully encapsulated in the microparticles.

Animal care

All animal studies were approved by the University of Minnesota Institutional Animal Care and Use Committee. Balb-*neu*T mice were bred according to established protocols [24, 25]. Mice were given access to food and water ad libitum. Genotyping was performed by Transnetyx Inc. (Cordova, TN) using tail snips collected at 1–3 weeks of age.

Pharmacokinetic studies

Balb/c mice (10–12 weeks old) were given a single subcutaneous (s.c.) injection of curcumin-loaded PLGA microparticles (equivalent to 58.2 mg of curcumin). A set of mice were sacrificed at various time points to collect blood and tissues. Mammary tissue was homogenized in distilled water using a handheld homogenizer (Omni International, Kennesaw, GA) and then lyophilized. Curcumin was extracted from the tissues with ethyl acetate (0.5 mL for whole blood, 2 mL for mammary tissue) overnight at room temperature. Samples were centrifuged at 3200×*g* for 10 min and the supernatant was dried under nitrogen stream. Curcumin was reconstituted in methanol and analyzed by liquid chromatography tandem mass spectroscopy (LC-MS/MS) using a previously published protocol [26].

Chromatography was performed on an Agilent Technologies 1200 series connected to a Thermo Scientific TSQ Quantum system operating in negative mode. An Agilent XDB-C18 1.8-μm, 4.6 × 50-mm column was used for separation. Mobile phase consisted of (A) 10 mM ammonium acetate and (B) acetonitrile. Linear gradient flow (0.5 mL/min) with a total run time of 10 min was used: 0–4.5 min, 45–100% B; 4.5–5.5 min, 100% B; 5.5–6 min, 100–45% B; 6–10 min, 45% B. The following mass transitions were monitored: curcumin—367 → 216, hydroxybenzophenone (internal standard)—197 → 92. Elution time was 4.3 min for curcumin and 3.4 min for hydroxybenzophenone. Curcumin produced a linear standard plot with a range from 0.013 to 1.25 μM and a R^2 >0.999.

Tumorigenesis studies

Female Balb-*neu*T mice were injected s.c. with curcumin-loaded PLGA microparticles (140 mg, corresponding to 58.2 mg of curcumin suspended in 750 μL sterile 1× PBS) or blank PLGA microparticles (90 mg) initially at 2, 4, 7, or 12 weeks of age and once a month thereafter. Curcumin has shown chemopreventive and anticancer potential in vitro in the dose range of 1–10 μM [27]. Our previous studies in mice show that curcumin is readily eliminated, with a total body clearance of ~3 L/kg/h [22, 23]. The relationship between clearance (CL), rate of drug input (R_0), and steady-state plasma concentration ($C_{ss} = R_0$/CL) can be used to calculate the curcumin delivery rate required to achieve a target plasma concentration of ~1 μM. Based on this relationship, a systemic delivery rate of ~1 mg/day is required to achieve a steady-state plasma concentration of 1 μM. Based on this, we estimated that 140 mg of the microparticles, corresponding to 58.2 mg of curcumin, will result in ~1 μM curcumin plasma levels. Mice treated initially at 2 weeks received a reduced dose (100 mg curcumin-loaded microparticles, 60 mg blank microparticles) to account for lower body weight. Microparticle dose was returned to normal beginning at 6 weeks of age in these mice. In control animals, saline was injected starting at 2 weeks (550 μL) and once a month thereafter (750 μL). Beginning at 8 weeks, mouse mammary pads were palpated once a week for tumors, with a 1-mm^3 mass considered as tumor formation. Volume of the right ventral anterior tumor was measured weekly using calipers. Volume was calculated as $V = (L \times W^2)/2$, where L is the tumor diameter parallel to the tail, and W is the tumor diameter perpendicular to the tail. Mice were euthanized when tumors in all ten mammary pads were detected.

Histology

Female Balb-*neu*T mice were s.c. injected with curcumin-loaded PLGA microparticles, blank PLGA microparticles, or saline as described above. Mice were sacrificed at 8 or 12 weeks of age and mammary tissue was harvested. A portion of the tissue was fixed with 10% buffered formalin for histology, while the other part was stored at −80 °C for Western blotting studies. Formalin-fixed mammary tissues were switched to 70% ethanol after 24 h. Tissue processing and staining for hematoxylin and eosin (H&E), Ki-67, and CD-31 were carried out by the Comparative Pathology Shared Resource at the University of Minnesota. All samples were received by the Comparative Pathology Shared Resource laboratory in 70% *v*/*v* ethanol/water, processed accordingly for routine histology, and embedded in paraffin. The samples were then cut into 4-μm sections and stained with H&E. Abnormal tissue areas (lobular hyperplasia, carcinoma in situ, and invasive carcinoma) were measured in ×10 magnification photographs using ImageJ software (Bethesda, MD). Ki-67 and CD-31 staining were quantified by taking 15–20 unique ×400 pictures per tissue and manually counting positively stained cells.

Western blotting

Mammary tissues were minced into fine pieces, and protein was extracted using 1× RIPA buffer. Protein content was determined using the BCA assay kit (Pierce, Rockford, IL). Western blotting was carried out using the Bio-Rad Criterion system (Hercules, CA). Proteins were separated by SDS-PAGE on a 4–15% polyacrylamide gradient gel and then transferred to a nitrocellulose membrane. Blots were probed with antibodies against HER-2, VEGF, or p65 NF-κB. β-Actin or β-tubulin served as loading controls. Bands were visualized with SuperSignal West Pico Chemiluminescent Substrate. Band intensities were determined using ImageJ and Origins (Northampton, MA) software.

Plasma and mammary tissue inflammatory cytokine levels

In a separate study, 12-week-old female BALB/c mice were injected with 750 μL saline or 90 mg blank PLGA microparticles and sacrificed after 24 h. Plasma and tissues were collected. Plasma was examined for IL-1β, IL-6, and TNF-α concentrations using ELISA kits (Invitrogen, Grand Island, NY) according to the manufacturer's protocol.

Lactic acid quantitation

Plasma lactic acid levels were determined using a lactic acid quantitation kit (Abnova, Walnut, CA) using a part of the tissues collected for the 1-month cytokine analysis described above. Plasma was used without additional processing.

Bioluminescence imaging

Transgenic mice carrying a NF-κB response element upstream of an inserted luciferase transgene (BALB/c-Tg[NF-κB-RE-luc]) were purchased from Taconic (Hudson, NY). These mice express luciferase when NF-κB is activated. Seven-week-old female mice were injected s.c. with saline or 90 mg empty PLGA microparticles, or given an i.p. injection of a 5% casein solution, as described in previous sections. Bioluminescence imaging was carried out on a Caliper LifeScience (Hopkinton, MA) IVIS® Spectrum instrument at various times after initiating treatment. Mice were injected i.p. with luciferin (150 mg/kg) 15 min before imaging. Data was analyzed using Living Image® software.

Endotoxin detection

Microparticles were tested for the presence of endotoxin using a LAL chromogenic endotoxin quantitation kit (Pierce). PLGA microparticles were suspended (120 mg/mL) in endotoxin-free water and vortexed. The microparticle suspension was centrifuged at 20,000×*g* for 10 min and the supernatant was tested directly.

Statistical analysis

Significance of observed differences was tested using Student's *t* test when applicable. Comparisons between more than two groups were carried out using ANOVA followed by Newman Keuls testing, with $p < 0.05$ being considered statistically significant.

Results

Formulation of curcumin microparticles and pharmacokinetic characterization

Curcumin-loaded microparticles were prepared by a modified solvent evaporation technique. Average particle diameter was 18.7 ± 7.7 μm (Fig. 1) with ~39% *w*/*w* (39 mg curcumin/100 mg microparticles) drug loading (78% encapsulation efficiency). These results are similar to that described for curcumin microparticles reported in previous studies [22, 23]. Empty PLGA (blank) microparticles were examined for endotoxin levels. The endotoxin levels were undetectable in microparticles (limit of quantitation = 0.1 endotoxin units/mL). A single injection of curcumin microparticles sustained blood (~0.2 μM) and mammary tissue (~1 μM) levels in BALB/c mice for up to 45 days (Fig. 2). Significantly higher blood and mammary tissue concentrations were observed 1 and 45 days after injection.

Curcumin microparticles delay tumorigenesis in Balb-*neu*T mice

The effect of beginning curcumin microparticle treatment at various stages of tumorigenesis was examined. In Balb-*neu*T mice initially injected with curcumin microparticles at 2 or 4 weeks of age and once a month thereafter, tumorigenesis was delayed compared to that in mice which received blank microparticles (Figs. 3a and 4a). Average time to first tumor was significantly delayed in mice initially receiving curcumin microparticles at 2 weeks (15.5 vs 14.2 weeks, $p < 0.05$) or 4 weeks (16.5 vs 14.4 weeks, $p < 0.05$) compared to empty microparticles (Figs. 3b and 4b). Time to reach 100% tumorigenesis was also delayed with curcumin microparticle treatment compared to blank microparticles in mice beginning treatment at 2 weeks (21.3 vs 18.5 weeks, $p < 0.05$) or 4 weeks (21.1 vs 19.1, $p < 0.05$). Rate of tumor growth in mice receiving curcumin microparticles initially at 2 weeks was significantly decreased compared to blank microparticle treatment (30.6 vs 77.6 mm^3/week, $p < 0.05$). Curcumin microparticle administration also significantly decreased abnormal mammary tissue area (Figs. 5 and 6).

Saline-treated controls developed tumors later than those receiving blank microparticles or curcumin microparticles (Figs. 3 and 4). Abnormal area was also significantly lower in saline-treated mice compared to that in other groups ($p < 0.05$). Mice that started receiving microparticle treatment at 7 or 12 weeks of age (after the onset of in situ carcinoma) showed no significant difference in tumorigenesis (data not shown).

Curcumin-loaded microparticles decrease HER-2 and VEGF protein levels and inhibit cell proliferation

Starting curcumin microparticle treatment at 2 or 4 weeks of age resulted in decreased HER-2 protein levels by 12 weeks of age (Fig. 7) but not by 8 weeks of age (data not shown). Ki-67 staining (marker for cell division) was not decreased in any treatment group receiving curcumin microparticles compared to blank microparticle controls. However, Ki-67 was substantially increased in mice receiving blank microparticles compared to saline controls, and this effect was somewhat reduced (not significant) in curcumin-loaded microparticles (Fig. 8).

VEGF levels were significantly decreased in curcumin microparticle treatment groups at 12 weeks of age (Fig. 9). Immunohistochemistry revealed a significant decrease in CD-31 staining (a marker for angiogenic microvasculature) in mice initially treated with curcumin microparticles at 2 weeks of age compared to blank microparticles (Fig. 10). Mice receiving curcumin microparticles at 4 weeks of age showed no significant difference in CD-31 staining compared to blank microparticles (not shown).

Saline controls showed significantly lower VEGF levels compared to both curcumin and blank microparticle treatment groups. Additionally, saline-treated animals showed significantly lower CD-31 staining at both 8 and 12 weeks of age. Total p65 NF-κB mammary tissue levels were not

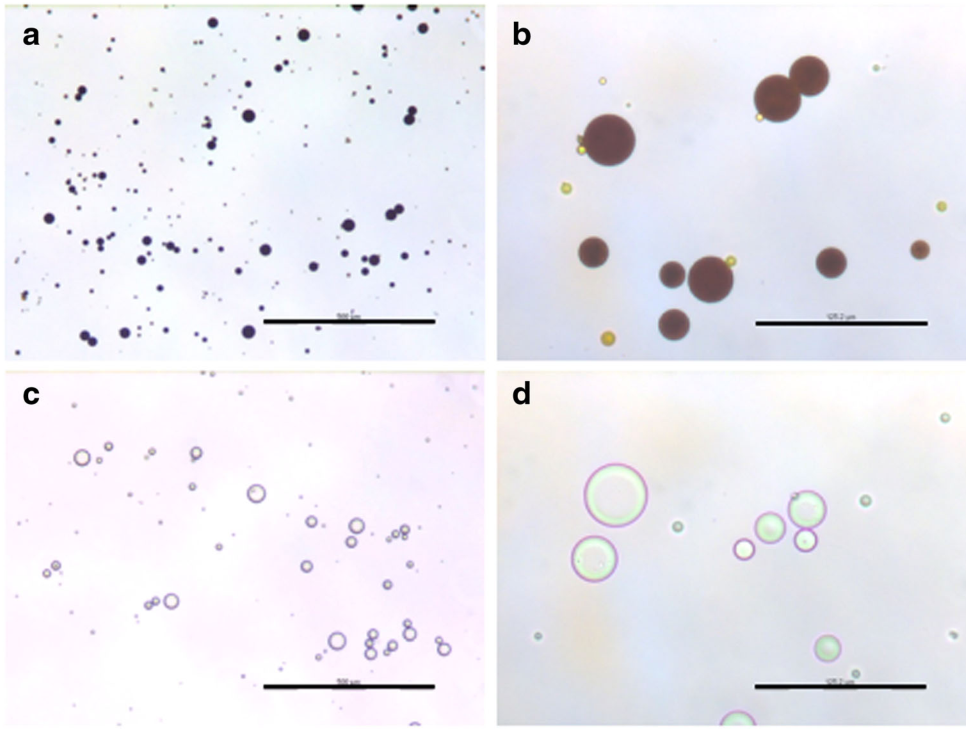

Fig. 1 Curcumin-loaded (**a**, **b**) or blank (**c**, **d**) microparticles were suspended in water and photographed using an optical microscope at ×100 (**a** and **c**, *scale bar* represents 500 μm) and ×400 (**b** and **d**, *scale bar* represents 125 μm) magnifications

significantly changed with curcumin microparticle treatment compared to blank microparticles (data not shown).

Lactic acid levels are increased in mice receiving PLGA microparticles

The excess lactic acid produced by PLGA microparticles may have contributed to the increase in VEGF and angiogenesis observed. Thus, the contribution of blank microparticles to circulating lactic acid was examined 1 month after injection. Treatment with blank microparticles resulted in significantly increased levels of lactic acid in plasma compared to that following saline treatment (Fig. 11).

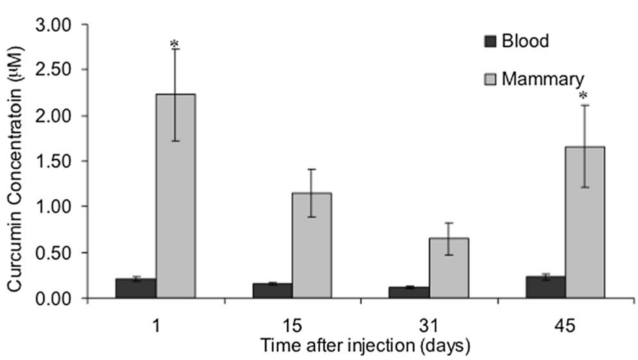

Fig. 2 Curcumin microparticles sustain blood and mammary curcumin levels for at least 45 days. Female BALB/c mice (n = 5–6) were administered a single dose of curcumin microparticles (equivalent to 58.2 mg of curcumin). A set of mice was sacrificed at various time points and tissues were collected and analyzed for curcumin content by LC-MS. Data are presented as average curcumin concentration ±SD. $^{*}p < 0.05$

Inflammation in mice receiving PLGA microparticles

NF-κB is the main regulator of acute and systemic inflammatory responses in the body. Activation of NF-κB was evaluated as a biomarker for systemic inflammation after PLGA microparticle injection. NF-κB-RE-luc mice express luciferase when NF-κB is activated. To determine if NF-κB was activated, mice were treated with blank microparticles. Introduction of blank microparticles significantly increased bioluminescence 2.4-fold ($p < 0.05$) compared to saline controls after 24 h, with NF-κB continuously activated for at least 72 h (Fig. 12).

In BALB/c mice, plasma IL-1β and IL-6 levels were significantly increased compared to saline controls 24 h after PLGA microparticle injection (Fig. 13). TNF-α levels were undetectable in plasma for both groups. No significant difference in IL-1α, IL-6, TNF-α, or GM-CSF was observed in plasma or mammary tissue 1 month after dosing (data not shown).

Discussion

Curcumin has been shown to affect several cellular pathways important in breast cancer [28, 29]. The wide array of curcumin effects is due in large part to the inhibition of IκB kinase [15, 16], resulting in reduced activation of NF-κB. This leads to a decrease in downstream activation of pathways important for inflammation and angiogenesis. In HER-2-positive tumor cells, curcumin has been shown to

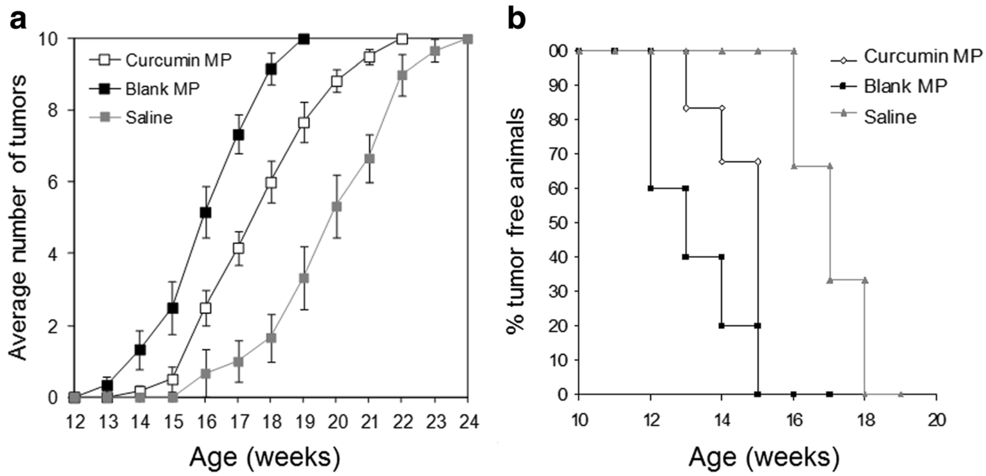

Fig. 3 Curcumin microparticles (*MP*) delay tumor appearance when initially injected at 2 weeks of age, but blank PLGA MP appear to accelerate the appearance of tumors. **a** Female Balb-*neu*T mice ($n = 6$) initially began receiving curcumin MP, empty MP injections, or saline once a month at 2 weeks of age. Data are presented as average number of palpable tumors present ± SE. **b** Time to first tumor was significantly delayed with curcumin MP treatment

deplete HER-2 protein levels in a time- and concentration-dependent manner [12, 13]. The concentration needed to deplete HER-2 by 50% was decreased from 40 to 10 μM by increasing the incubation time by just 12 h. We hypothesized that low, sustained levels of curcumin would also be effective in inhibiting HER-2-positive breast cancer in vivo.

The therapeutic usefulness of curcumin is limited by its poor solubility and bioavailability, which is due to poor absorption and extensive gut and hepatic metabolism [30–32]. To bypass these problems, curcumin-loaded PLGA microparticles capable of sustaining blood and mammary tissue levels for at least 45 days after a single injection were formulated. The significantly higher curcumin concentration in the blood and mammary tissue 1 day after administration is likely due to burst release typically seen in implants. Drug residing at or near the surface of microparticles has very little diffusional barrier and is therefore released quickly. Previous in vitro release studies using this curcumin microparticle formulation showed 10% drug release within 24 h [22, 23]. Tissue levels of curcumin were steady in the interim, agreeing well with the zero order release profiles observed in the in vitro release experiments [22, 23]. Forty-five days after administration, a similar second burst release occurs likely due to the extensive degradation of the polymer [33].

The transgenic Balb-*neu*T mouse model was used to examine the efficacy of curcumin chemoprevention. The Balb-*neu*T model overexpresses neu protein via the MMTV-LTR promoter. The overexpressed protein is an activated form (*neu*T), which allows for signal transduction even in the absence of signaling molecules [34]. The model is aggressive, with hyperplasia appearing as early as 3 weeks after birth, coinciding with initial mammary development. Microvasculature is increased from 4 to 6 weeks, with in situ carcinoma appearing around 7 weeks. By 17 weeks, at least one palpable tumor is present in the mouse. This mouse model thus allows for evaluating the effect of time of curcumin intervention on tumor progression.

Initiating curcumin treatment at 2 or 4 weeks of age, but not at 7 or 12 weeks of age (not shown), delayed the tumor onset compared to the blank microparticle treatment group. When these results were compared to saline controls, the outcome was very surprising. The time to first tumor and the overall tumorigenesis in saline-treated mice were slower than in the

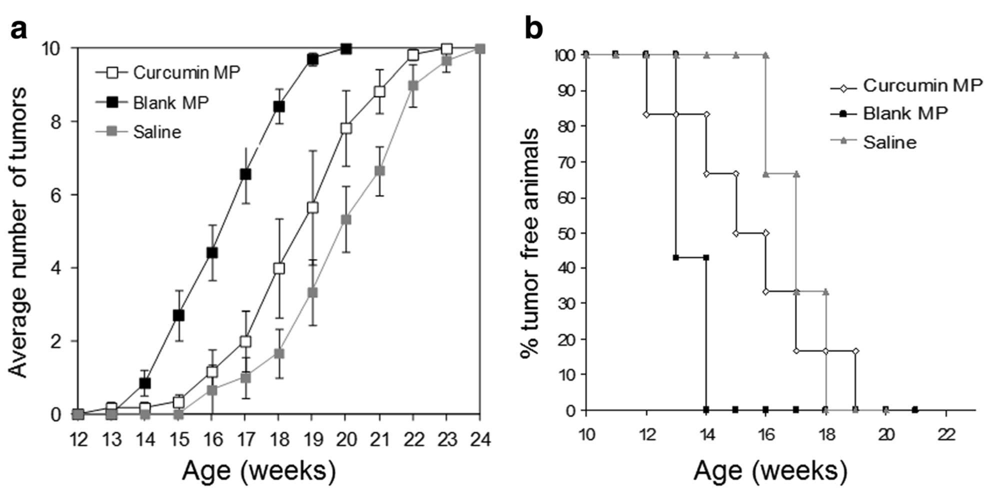

Fig. 4 Curcumin microparticles (*MP*) delay tumor appearance when initially injected at 4 weeks of age, but blank PLGA MP appear to accelerate the appearance of tumors. **a** Female Balb-*neu*T mice ($n = 6$) initially began receiving curcumin MP, empty MP injections, or saline once a month at 4 weeks of age. Data are presented as average number of palpable tumors present ± SE. **b** Time to first tumor was significantly delayed with curcumin MP treatment

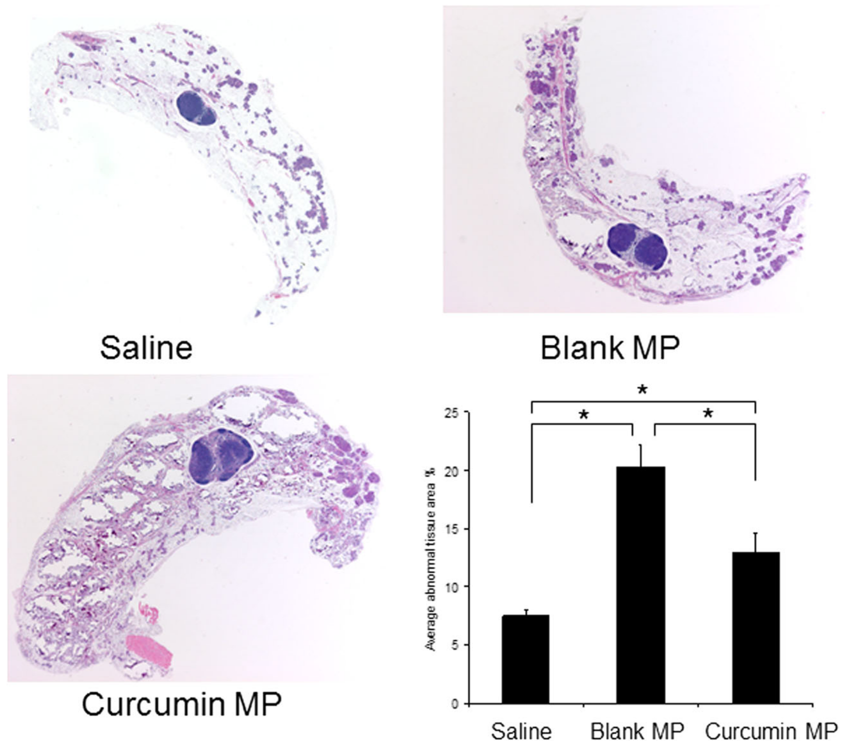

Fig. 5 Curcumin microparticle (*MP*) treatment reduces abnormal tissue area in Balb-*neu*T mice initially treated at 2 weeks of age; ×10 magnification of H&E-stained mammary tissues taken from 12-week-old female Balb-*neu*T mice ($n = 4$) after 10 weeks of curcumin MP, blank PLGA MP, or saline administration. Abnormal tissue was quantified using ImageJ software. Data are presented as average abnormal tissue area ±SD. *$p < 0.05$

other treatment groups. This suggested that blank microparticles accelerated tumorigenesis in this model, and curcumin inhibited this effect. Previous in vitro studies using PLGA particles showed no significant cytotoxicity. The acute local inflammatory effects of PLGA microparticles are well established [35, 36], but no previous studies have reported systemic inflammation.

It was interesting to note that average time for first tumor was 15.5 weeks when curcumin treatment was started at 2 weeks, whereas it was 16.5 weeks when the treatment was started at 4 weeks of age. The reason for this counterintuitive result is not clear since one would expect earlier intervention to have a greater benefit. However, it is possible that the protection offered by

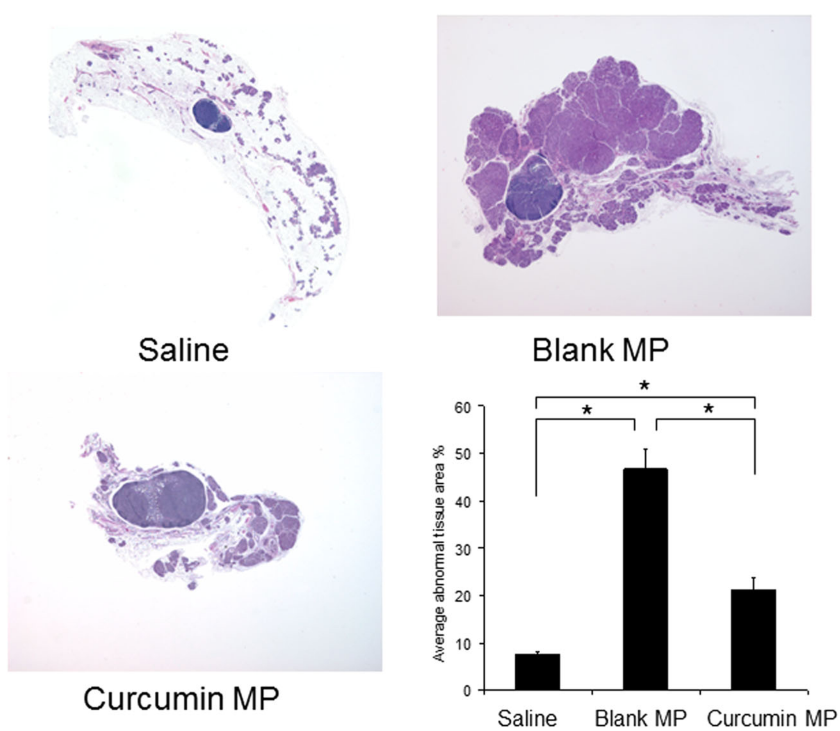

Fig. 6 Curcumin microparticle (*MP*) treatment reduces abnormal tissue area in Balb-*neu*T mice initially treated at 4 weeks of age; ×10 magnification of H&E-stained mammary tissues taken from 12-week-old female Balb-neuT mice ($n = 4$) after 8 weeks of curcumin MP, blank PLGA MP, or saline administration. Abnormal tissue was quantified using ImageJ software. Data are presented as average abnormal tissue area ±SD. *$p < 0.05$

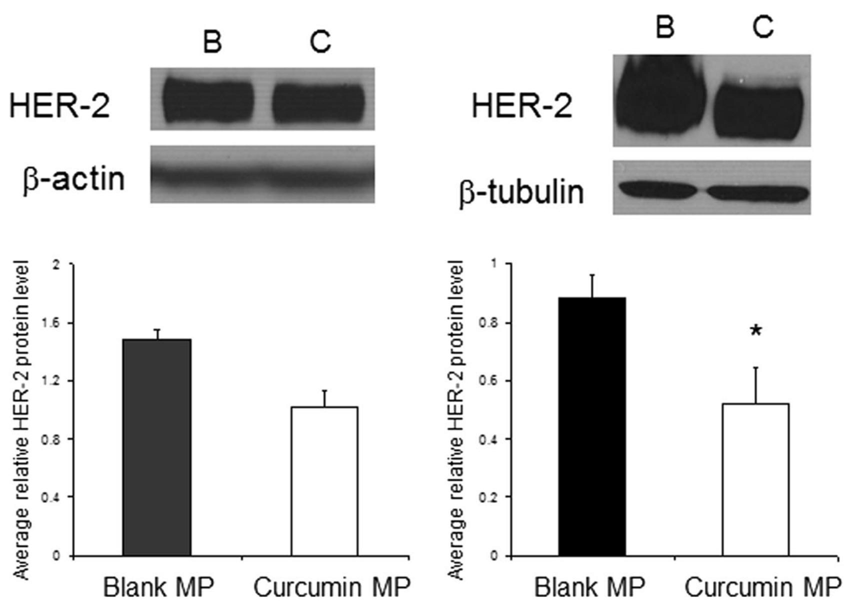

Fig. 7 Curcumin-loaded microparticles (*MP*) decrease mammary HER-2 protein levels. Female BALB-*neu*T mice ($n = 2$–4) began receiving curcumin MP (*C*) or blank MP (*B*) at 2 (*left*) or 4 (*right*) weeks, then once a month thereafter. Mice were sacrificed at 12 weeks and mammary tissue was harvested. Proteins were separated by SDS-PAGE then transferred to a nitrocellulose blot. β-Actin and β-tubulin served as loading controls. Data are presented as average relative protein level ±SD. *$p < 0.05$ compared to blank MP control

curcumin is not as impactful as the inflammation induced by PLGA in these young mice.

NF-κB is the major pathway for acute and systemic inflammation [37, 38]. Activation of the NF-κB pathway in macrophages leads to the release of proinflammatory cytokines such as IL-1β, IL-6, and TNF-α. Therefore, activation of this pathway would be a likely player in any inflammatory effects induced by blank microparticles. Bioluminescence in NF-κB-RE-luc mice was increased 2.4-fold in mice treated with blank microparticles. NF-κB activation was significantly elevated compared to saline controls for at least 72 h but was near background 1 week after dosing. Additionally, IL-1β and IL-6 plasma levels were significantly higher in mice 24 h after blank microparticle injection. Based on this data, it is likely that introduction of blank microparticles leads to mild systemic inflammation via ubiquitous activation of NF-κB. The microparticles used for all the studies were made with endotoxin-free water to prevent any bacterial contamination. Confirmation that microparticles are devoid of endotoxins prior to injection further supports that NF-κB activation was not a by-product of contamination during microparticle fabrication. No significant difference in inflammatory cytokine (IL-1α, IL-6, TNF-α, GM-CSF) levels was seen 1 month after injection with blank microparticles compared to saline control. It is likely that the

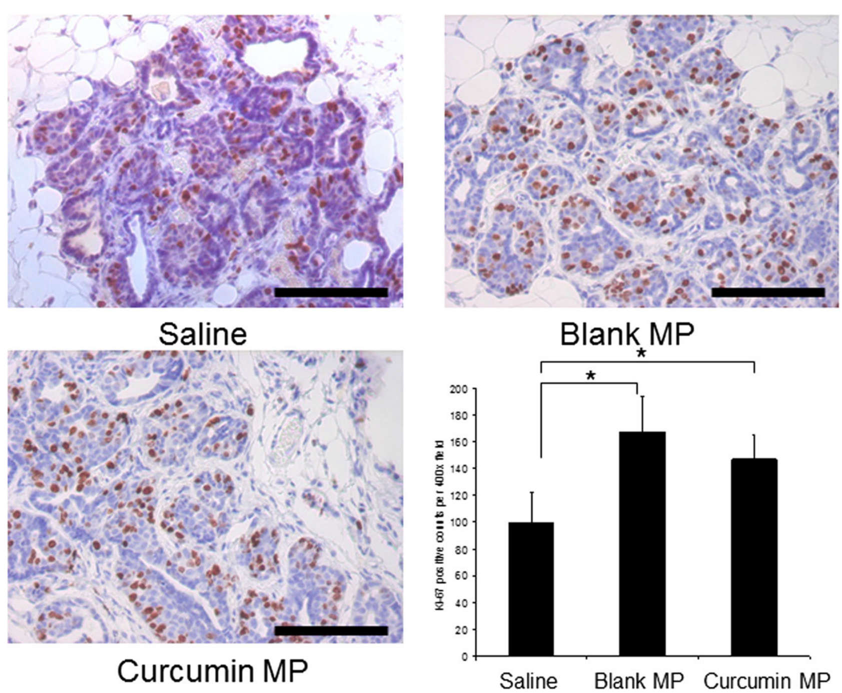

Fig. 8 Effect of curcumin microparticles (*MP*) on tumor cell proliferation. Female BALB-*neu*T mice were initially treated with saline, curcumin MP, or blank MP beginning at 2 weeks of age. Mice were sacrificed at 12 weeks of age and mammary tissue was harvested and stained with anti-Ki-67 antibody. Positive Ki-67 staining was manually counted using 15–20 individual ×400 magnification pictures. *Black bars* represent 100 μm. Data are presented as average number of Ki-67-positive counts per a ×400 field ±SD. *$p < 0.05$

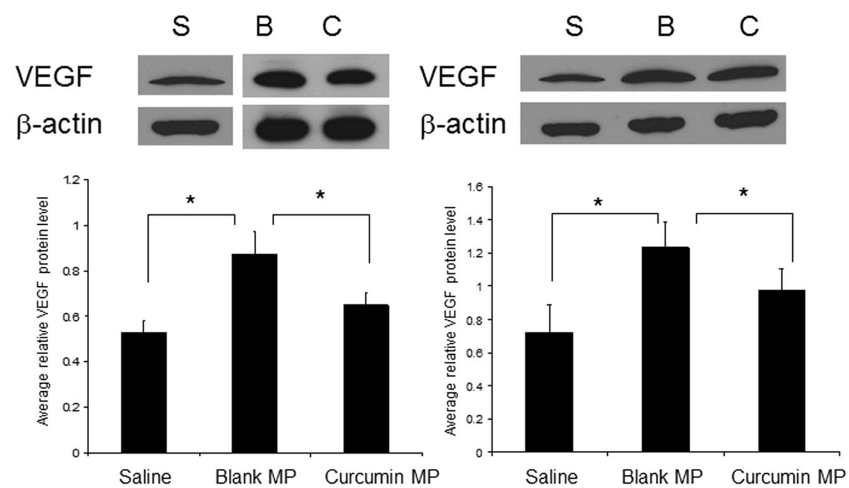

Fig. 9 Effect of curcumin and empty PLGA microparticles (*MP*) on tumor VEGF levels compared to saline controls. Female Balb-*neu*T mice began receiving curcumin MP (*C*), blank MP (*B*), or saline injections (*S*) at 2 (*left*) or 4 (*right*) weeks of age and were sacrificed at 12 weeks of age. Protein extracts were separated by SDS-PAGE and probed for VEGF protein. Data are presented as average protein level relative to β-actin ±SD. **p* < 0.05

systemic inflammation had subsided 1 month after microparticle injection, as evident by the lack of NF-κB activation at 7 days postdose. Curcumin is a known anti-inflammatory agent and has been shown to block the activation of NF-κB. It is possible that curcumin microparticle treatment offset the systemic inflammation caused by PLGA microparticles and this led to the observed delay in tumorigenesis.

Alternatively, lactic acid (existing as lactate in physiologic pH) can act as a signaling molecule during tumorigenesis. In developing tumors, pH is reduced due to excessive lactic acid produced from tumor cells. This is a by-product of the Warburg effect, observed when tumor cells switch from oxidative phosphorylation to glycolysis as their main ATP pathway [39, 40]. Lactic acid is exported by tumor cells via monocarboxylate transporter-4 (MCT-4) into the extracellular matrix. Excess lactate in the extracellular matrix has two fates. Lactate can be taken up by other tumor cells via the MCT-1 transporter and used to produce energy. This allows for faster tumor growth, as well as decreased glucose reliance. The glucose not taken up by these cells is free to diffuse farther into the tumor and provide energy for otherwise hypoxic cells. Additionally, lactate can activate NF-κB in endothelial cells and lead to IL-8 production [41]. Excess lactate has been shown to increase HIF-1α concentration, stimulating angiogenesis [42].

Our studies show that the systemic lactic acid concentration was slightly elevated in animals that received blank microparticles. Excess lactate could lead to increased tumor growth and thus produce a faster time to palpable tumors. Increased systemic lactate could also be taken up by endothelial cells already stimulated by the increased inflammation seen in this model, leading to enhanced angiogenesis. Tumorigenesis in this mouse model is initially driven by inflammation with

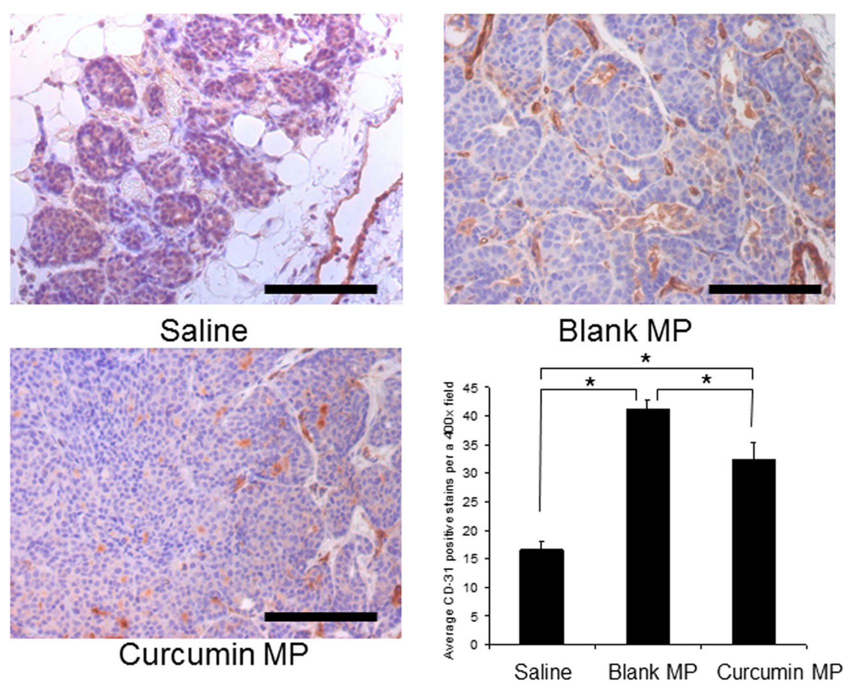

Fig. 10 Effect of curcumin and empty PLGA microparticles (*MP*) on microvasculature in mammary tissues of BALB-*neu*T mice compared to saline controls. Female BALB-*neu*T mice were initially treated with saline, curcumin MP, or blank MP beginning at 2 weeks of age. Mice were sacrificed at 12 weeks of age and mammary tissue was stained with anti-CD-31 antibody. CD-31 staining was manually counted using 15–20 individual ×400 magnification pictures. *Black bars* represent 100 μm. Data are presented as average number of CD-31-positive counts per a ×400 field ±SD. **p* < 0.05

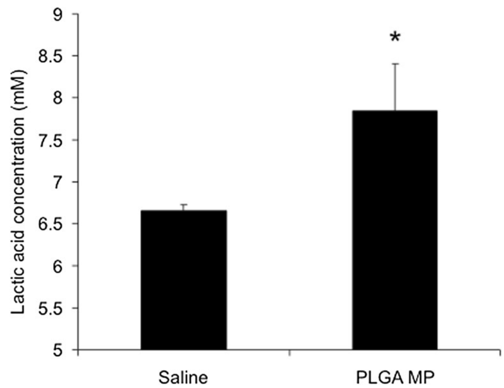

Fig. 11 PLGA microparticles increase lactic acid levels in plasma. Female BALB-*neu*T mice were administered PLGA microparticles at 2 weeks of age. After 1 month, mice were sacrificed and blood was collected. Plasma lactic acid levels were determined using a lactate assay kit. Data are presented as average lactic acid concentration ±SD. $*p < 0.05$, compared to saline-injected control

neoangiogenesis ending by 6 weeks of age. No difference in outcome was seen when microparticles were introduced after the angiogenic switch (mice injected at 7 or 12 weeks) and tumor growth was being driven solely by HER-2 overexpression. Western blotting confirmed that blank microparticle treatment increased VEGF levels. Similarly, immunohistochemistry studies showed that CD-31-positive blood vessels were increased in mice receiving PLGA microparticles, although the effect was more pronounced in mice beginning treatment at 2 weeks. Induction of VEGF and angiogenesis by lactate is well established, and these results further support the hypothesis that excess lactate produced by PLGA could contribute to enhanced angiogenesis and tumorigenesis in this model.

Curcumin showed bioactivity in the Balb-*neu*T mice, although it could not completely overcome the apparent tumorigenic effects of blank microparticles. In mice receiving

Fig. 12 PLGA microparticles (*MP*) induce NF-κB activation in vivo. Female NF-κB-RE luc mice ($n = 3$) were injected with saline or 90 mg PLGA microparticles and imaged at various time points after injection. **a** Mice were administered luciferin (150 mg/kg) 15 min prior to imaging. **b** Bioluminescence was calculated using Living Image software and values were compared. Data are presented as individual photon flux measurements (photons/s). $p < 0.05$

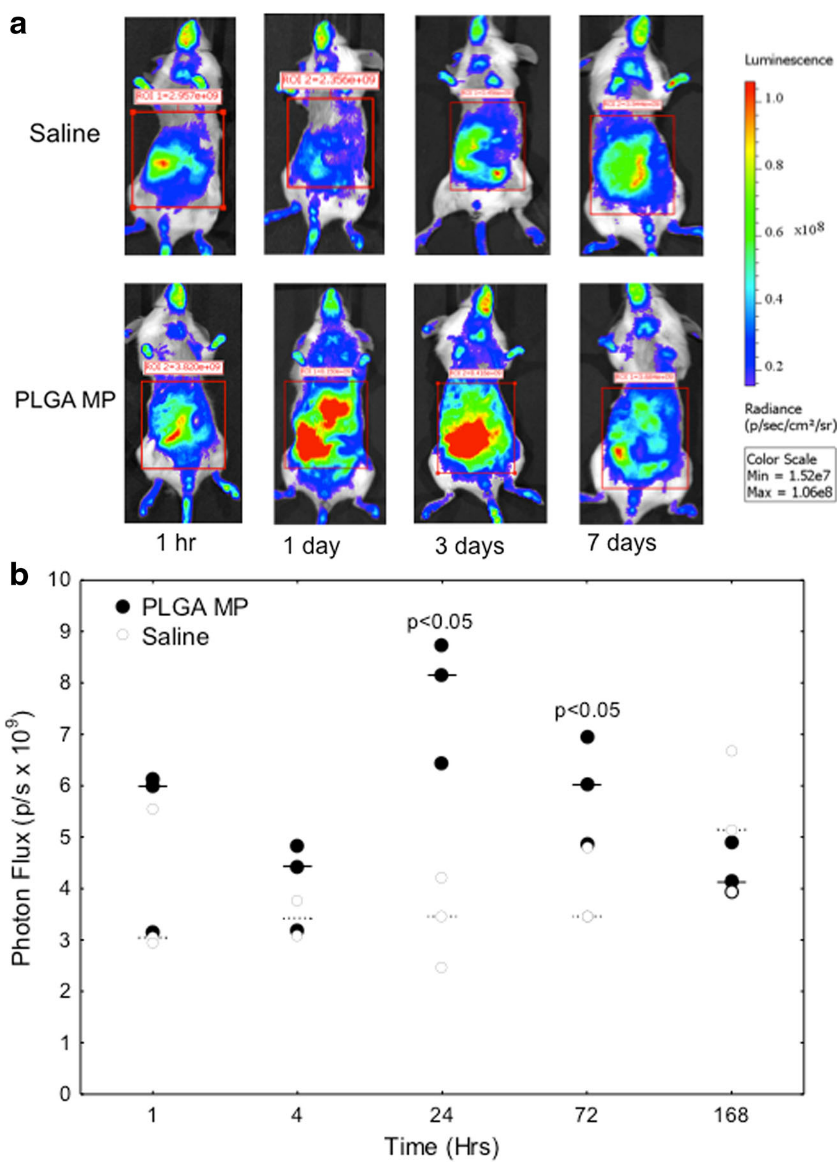

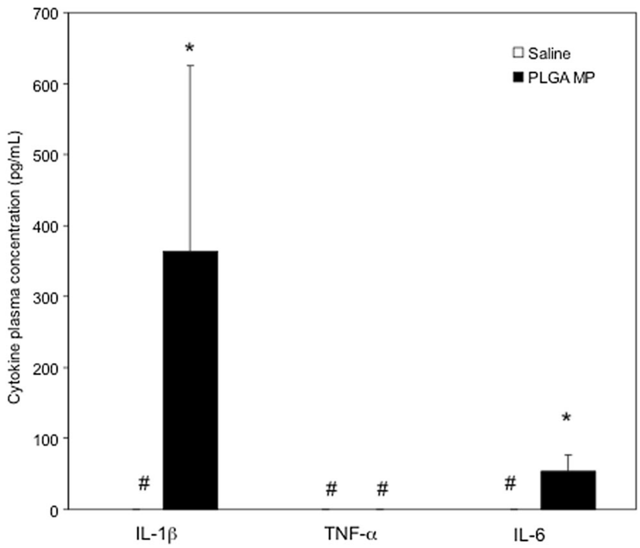

Fig. 13 PLGA microparticles (*MP*) increase plasma inflammatory cytokine levels. Female BALB/c mice were administered saline or 90 mg PLGA MP and sacrificed after 24 h. Cytokine levels were determined by ELISA. **p* < 0.05. #, values were below the detection limit of the ELISA kit

curcumin microparticles, abnormal tissue area was significantly decreased compared to those receiving blank microparticles. At 12 weeks of age, curcumin microparticle-treated mice had decreased HER-2 protein levels. While additional comparisons with untreated and free curcumin-treated controls are needed, this data provides preliminary support for the hypothesis that low, steady curcumin levels could result in significant changes in cellular pathways. Previous studies using curcumin and other dietary polyphenols at sustained low doses showed similar effects [43]. HER-2 is the main driver of tumorigenesis in this model, and its depletion is linked to decreased growth. However, the excess lactic acid may have offset the antiproliferative effects of curcumin which would explain why Ki-67 staining was not significantly changed by curcumin microparticle treatment but was significantly increased with blank MP treatment. Additionally, it is possible that the presence of curcumin in microparticles had an inhibitory effect on the hydrolysis of PLGA, resulting in slower lactic acid release, and, therefore, a decrease in tumorigenesis. Further studies examining the differences in the degradation rates and lactic acid production between curcumin microparticles and blank microparticles are needed to confirm this mechanism.

PLGA microparticles have been shown to be safe and have been used in the clinic for several years. Our previous in vitro studies have shown that blank PLGA particle formulations do not cause any cytotoxicity to mammalian cells [44, 45]. The in vivo side effects (systemic inflammation, increased angiogenesis) of PLGA microparticles seen in this study can be ascribed to the high dose used here. The dose of PLGA microparticles used here was higher than what is typically used in the clinic (60–90 mg/mouse vs ~2 g/patient) but is in the range that is used in preclinical studies (20–150 mg/mouse; [46–49]). These high microparticle doses were necessitated by the need for micromolar tissue concentrations and the short half-life of curcumin. Our studies suggest that the effect of formulation excipients used needs careful consideration, especially when used at high doses and for prolonged periods of time. Interestingly, a recent report showed that regular consumption of dietary emulsifiers, carboxymethylcellulose or polysorbate-80, exacerbated colorectal tumor development [50], pointing to other instances where excipients can induce undesirable chronic side effects.

Our studies suggest that sustained tissue levels of curcumin can inhibit tumorigenesis. However, its low potency and rapid systemic elimination are impediments to the development of a clinically translatable sustained release dosage form. Approaches that can decrease the overall dose of curcumin (for example, by increasing its potency [51–53] or reducing its clearance rate [54, 55]) may allow the development of formulations suitable for cancer chemoprevention.

Conclusions

Curcumin microparticles were effective in delaying tumorigenesis in Balb-*neu*T mice compared to blank PLGA microparticle controls. However, when compared to saline control, PLGA microparticles were shown to accelerate tumorigenesis. Future studies should examine this effect in depth, as well as evaluate other formulations and modalities of curcumin for cancer chemoprevention.

Acknowledgements This study received funding from the National Institutes of Health (CA 141996) and Grant-In-Aid program of the University of Minnesota.

Compliance with ethical standards All institutional and national guidelines for the care and use of laboratory animals were followed.

Conflict of interest The authors declare that they have no conflict of interest.

References

1. Hynes NE, MacDonald G. ErbB receptors and signaling pathways in cancer. Curr Opin Cell Biol. 2009;21:177–84.
2. Yarden Y. Biology of HER2 and its importance in breast cancer. Oncology. 2001;61(Suppl 2):1–13.
3. Tai W, Mahato R, Cheng K. The role of HER2 in cancer therapy and targeted drug delivery. J Control Release. 2010;146:264–75.
4. Korkaya H, Paulson A, Iovino F, Wicha MS. HER2 regulates the mammary stem/progenitor cell population driving tumorigenesis and invasion. Oncogene. 2008;27:6120–30.
5. Sorlie T. Molecular portraits of breast cancer: tumour subtypes as distinct disease entities. Eur J Cancer. 2004;40:2667–75.

6. Geyer CE, Forster J, Lindquist D, Chan S, Romieu CG, Pienkowski T, Jagiello-Gruszfeld A, Crown J, Chan A, Kaufman B, Skarlos D, Campone M, Davidson N, Berger M, Oliva C, Rubin SD, Stein S, Cameron D. Lapatinib plus capecitabine for HER2-positive advanced breast cancer. N Engl J Med. 2006;355:2733–43.
7. Baselga J, Perez EA, Pienkowski T, Bell R. Adjuvant trastuzumab: a milestone in the treatment of HER-2-positive early breast cancer. Oncologist. 2006;11(Suppl 1):4–12.
8. Ryan Q, Ibrahim A, Cohen MH, Johnson J, Ko CW, Sridhara R, Justice R, Pazdur R. FDA drug approval summary: lapatinib in combination with capecitabine for previously treated metastatic breast cancer that overexpresses HER-2. Oncologist. 2008;13: 1114–9.
9. Bendell JC, Domchek SM, Burstein HJ, Harris L, Younger J, Kuter I, Bunnell C, Rue M, Gelman R, Winer E. Central nervous system metastases in women who receive trastuzumab-based therapy for metastatic breast carcinoma. Cancer. 2003;97:2972–7.
10. Polli JW, Olson KL, Chism JP, John-Williams LS, Yeager RL, Woodard SM, Otto V, Castellino S, Demby VE. An unexpected synergist role of P-glycoprotein and breast cancer resistance protein on the central nervous system penetration of the tyrosine kinase inhibitor lapatinib (N-{3-chloro-4-[(3-fluorobenzyl)oxy]phenyl}-6-[5-({[2-(methylsulfonyl)ethyl]amino }methyl)-2-furyl]-4-quinazolinamine; GW572016). Drug Metab Dispos. 2009;37: 439–42.
11. Gonzalez-Angulo AM, Litton JK, Broglio KR, Meric-Bernstam F, Rakkhit R, Cardoso F, Peintinger F, Hanrahan EO, Sahin A, Guray M, Larsimont D, Feoli F, Stranzl H, Buchholz TA, Valero V, Theriault R, Piccart-Gebhart M, Ravdin PM, Berry DA, Hortobagyi GN. High risk of recurrence for patients with breast cancer who have human epidermal growth factor receptor 2-positive, node-negative tumors 1 cm or smaller. J Clin Oncol. 2009;27: 5700–6.
12. Hong RL, Spohn WH, Hung MC. Curcumin inhibits tyrosine kinase activity of p185neu and also depletes p185neu. Clin Cancer Res. 1999;5:1884–91.
13. Jung Y, Xu W, Kim H, Ha N, Neckers L. Curcumin-induced degradation of ErbB2: a role for the E3 ubiquitin ligase CHIP and the Michael reaction acceptor activity of curcumin. Biochim Biophys Acta. 2007;1773:383–90.
14. Goel A, Kunnumakkara AB, Aggarwal BB. Curcumin as "curecumin": from kitchen to clinic. Biochem Pharmacol. 2008;75:787–809.
15. Jobin C, Bradham CA, Russo MP, Juma B, Narula AS, Brenner DA, Sartor RB. Curcumin blocks cytokine-mediated NF-kappa B activation and proinflammatory gene expression by inhibiting inhibitory factor I-kappa B kinase activity. J Immunol. 1999;163: 3474–83.
16. Biswas SK, McClure D, Jimenez LA, Megson IL, Rahman I. Curcumin induces glutathione biosynthesis and inhibits NF-kappaB activation and interleukin-8 release in alveolar epithelial cells: mechanism of free radical scavenging activity. Antioxid Redox Signal. 2005;7:32–41.
17. Anand P, Kunnumakkara AB, Newman RA, Aggarwal BB. Bioavailability of curcumin: problems and promises. Mol Pharm. 2007;4:807–18.
18. Benny O, Menon LG, Ariel G, Goren E, Kim SK, Stewman C, Black PM, Carroll RS, Machluf M. Local delivery of poly lactic-co-glycolic acid microspheres containing imatinib mesylate inhibits intracranial xenograft glioma growth. Clin Cancer Res. 2009;15: 1222–31.
19. Mundargi RC, Babu VR, Rangaswamy V, Patel P, Aminabhavi TM. Nano/micro technologies for delivering macromolecular therapeutics using poly (D,L-lactide-co-glycolide) and its derivatives. J Control Release. 2008;125:193–209.
20. Freiberg S, Zhu XX. Polymer microspheres for controlled drug release. Int J Pharm. 2004;282:1–18.
21. Wischke C, Schwendeman SP. Principles of encapsulating hydrophobic drugs in PLA/PLGA microparticles. Int J Pharm. 2008;364: 298–327.
22. Shahani K, Panyam J. Highly loaded, sustained-release microparticles of curcumin for chemoprevention. J Pharm Sci. 2011;100: 2599–609.
23. Shahani K, Swaminathan SK, Freeman D, Blum A, Ma L, Panyam J. Injectable sustained release microparticles of curcumin: a new concept for cancer chemoprevention. Cancer Res. 2010;70:4443–52.
24. Boggio K, Di Carlo E, Rovero S, Cavallo F, Quaglino E, Lollini PL, Nanni P, Nicoletti G, Wolf S, Musiani P, Forni G. Ability of systemic interleukin-12 to hamper progressive stages of mammary carcinogenesis in HER2/neu transgenic mice. Cancer Res. 2000;60:359–64.
25. Boggio K, Nicoletti G, Di Carlo E, Cavallo F, Landuzzi L, Melani C, Giovarelli M, Rossi I, Nanni P, De Giovanni C, Bouchard P, Wolf S, Modesti A, Musiani P, Lollini PL, Colombo MP, Forni G. Interleukin 12-mediated prevention of spontaneous mammary adenocarcinomas in two lines of Her-2/neu transgenic mice. J Exp Med. 1998;188:589–96.
26. Schaefers MM, Breshears LM, Anderson MJ, Lin YC, Grill AE, Panyam J, Southern PJ, Schlievert PM, Peterson ML. Epithelial proinflammatory response and curcumin-mediated protection from staphylococcal toxic shock syndrome toxin-1. PLoS One. 2012;7: e32813.
27. Garcea G, Jones DJ, Singh R, Dennison AR, Farmer PB, Sharma RA, Steward WP, Gescher AJ, Berry DP. Detection of curcumin and its metabolites in hepatic tissue and portal blood of patients following oral administration. Br J Cancer. 2004;90:1011–5.
28. Anand P, Sundaram C, Jhurani S, Kunnumakkara AB, Aggarwal BB. Curcumin and cancer: an "old-age" disease with an "age-old" solution. Cancer Lett. 2008;267:133–64.
29. Rowe DL, Ozbay T, O'Regan RM, Nahta R. Modulation of the BRCA1 protein and induction of apoptosis in triple negative breast cancer cell lines by the polyphenolic compound curcumin. Breast Cancer (Auckl). 2009;3:61–75.
30. Pan MH, Huang TM, Lin JK. Biotransformation of curcumin through reduction and glucuronidation in mice. Drug Metab Dispos. 1999;27:486–94.
31. Sharma RA, Steward WP, Gescher AJ. Pharmacokinetics and pharmacodynamics of curcumin. Adv Exp Med Biol. 2007;595:453–70.
32. Sharma RA, Euden SA, Platton SL, Cooke DN, Shafayat A, Hewitt HR, Marczylo TH, Morgan B, Hemingway D, Plummer SM, Pirmohamed M, Gescher AJ, Steward WP. Phase I clinical trial of oral curcumin: biomarkers of systemic activity and compliance. Clin Cancer Res. 2004;10:6847–54.
33. Panyam J, Dali MM, Sahoo SK, Ma W, Chakravarthi SS, Amidon GL, Levy RJ, Labhasetwar V. Polymer degradation and in vitro release of a model protein from poly (d,l-lactide-co-glycolide) nano- and microparticles. J Control Release. 2003;92:173–87.
34. Quaglino E, Mastini C, Forni G, Cavallo F. ErbB2 transgenic mice: a tool for investigation of the immune prevention and treatment of mammary carcinomas. Curr Protoc Immunol. 2008;Chapter 20: Unit 20 29 21—10.
35. Fournier E, Passirani C, Montero-Menei CN, Benoit JP. Biocompatibility of implantable synthetic polymeric drug carriers: focus on brain biocompatibility. Biomaterials. 2003;24:3311–31.
36. Shive MS, Anderson JM. Biodegradation and biocompatibility of PLA and PLGA microspheres. Adv Drug Deliv Rev. 1997;28:5–24.
37. Karin M. Nuclear factor-kappaB in cancer development and progression. Nature. 2006;441:431–6.

38. Beutler B. Tlr4: central component of the sole mammalian LPS sensor. Curr Opin Immunol. 2000;12:20–6.
39. Draoui N, Feron O. Lactate shuttles at a glance: from physiological paradigms to anti-cancer treatments. Dis Model Mech. 2011;4:727–32.
40. Semenza GL. Tumor metabolism: cancer cells give and take lactate. J Clin Invest. 2008;118:3835–7.
41. Vegran F, Boidot R, Michiels C, Sonveaux P, Feron O. Lactate influx through the endothelial cell monocarboxylate transporter MCT1 supports an NF-kappaB/IL-8 pathway that drives tumor angiogenesis. Cancer Res. 2011;71:2550–60.
42. Sonveaux P, Copetti T, De Saedeleer CJ, Vegran F, Verrax J, Kennedy KM, Moon EJ, Dhup S, Danhier P, Frerart F, Gallez B, Ribeiro A, Michiels C, Dewhirst MW, Feron O. Targeting the lactate transporter MCT1 in endothelial cells inhibits lactate-induced HIF-1 activation and tumor angiogenesis. PLoS One. 2012;7:e33418.
43. Moiseeva EP, Almeida GM, Jones GD, Manson MM. Extended treatment with physiologic concentrations of dietary phytochemicals results in altered gene expression, reduced growth, and apoptosis of cancer cells. Mol Cancer Ther. 2007;6:3071–9.
44. Panyam J, Zhou WZ, Prabha S, Sahoo SK, Labhasetwar V. Rapid endo-lysosomal escape of poly(DL-lactide-co-glycolide) nanoparticles: implications for drug and gene delivery. FASEB J. 2002;16:1217–26.
45. Patil Y, Sadhukha T, Ma L, Panyam J. Nanoparticle-mediated simultaneous and targeted delivery of paclitaxel and tariquidar overcomes tumor drug resistance. J Control Release. 2009;136:21–9.
46. Kang SW, La WG, Kim BS. Open macroporous poly(lactic-co-glycolic acid) microspheres as an injectable scaffold for cartilage tissue engineering. J Biomater Sci Polym Ed. 2009;20:399–409.
47. Negrín CM, Delgado A, Llabrés M, Évora C. In vivo–in vitro study of biodegradable methadone delivery systems. Biomaterials. 2001;22:563–70.
48. Negrín CM, Delgado A, Llabrés M, Évora C. Methadone implants for methadone maintenance treatment. In vitro and in vivo animal studies. J Control Release. 2004;95:413–21.
49. Rabin C, Liang Y, Ehrlichman RS, Budhian A, Metzger KL, Majewski-Tiedeken C, Winey KI, Siegel SJ. In vitro and in vivo demonstration of risperidone implants in mice. Schizophr Res. 2008;98:66–78.
50. Viennois E, Merlin D, Gewirtz AT, Chassaing B. Dietary emulsifier-induced low-grade inflammation promotes colon carcinogenesis. Cancer Res. 2017;77:27–40.
51. Shijun Z, Terry WM, Nao M, Randy BH, Richard FA, Prabhakar R, Taylor JE, Hongzheng Z, Gabriel S, Zhuo GC, Aiming S, Haian F, Fadlo RK, Dong MS, James PS, Mamoru S. Synthetic curcumin analog UBS109 inhibits the growth of head and neck squamous cell carcinoma xenografts. Curr Cancer Drug Targets. 2014;14:380–93.
52. Wang R, Chen C, Zhang X, Zhang C, Zhong Q, Chen G, Zhang Q, Zheng S, Wang G, Chen Q-H. Structure–activity relationship and pharmacokinetic studies of 1,5-diheteroarylpenta-1,4-dien-3-ones: a class of promising curcumin-based anticancer agents. J Med Chem. 2015;58:4713–26.
53. Wang R, Zhang X, Chen C, Chen G, Zhong Q, Zhang Q, Zheng S, Wang G, Chen Q-H. Synthesis and evaluation of 1,7-diheteroarylhepta-1,4,6-trien-3-ones as curcumin-based anticancer agents. Eur J Med Chem. 2016;110:164–80.
54. Grill AE, Koniar B, Panyam J. Co-delivery of natural metabolic inhibitors in a self-microemulsifying drug delivery system for improved oral bioavailability of curcumin. Drug Deliv Transl Res. 2014;4:344–52.
55. Li S, Fang C, Zhang J, Liu B, Wei Z, Fan X, Sui Z, Tan Q. Catanionic lipid nanosystems improve pharmacokinetics and anti-lung cancer activity of curcumin. Nanomedicine. 2016;12:1567–79.